A new framework for the optimal management of urban runoff with low-impact development stormwater control measures considering service-performance reduction

Melika Mani, Omid Bozorg-Haddad and Hugo A. Loáiciga

ABSTRACT

This paper presents a comprehensive framework for the quantitative management of urban runoff. The framework assesses the response of urban catchments to design rainfall events and identifies low-impact development (LID) stormwater control measures (SCMs) for runoff control and flood mitigation. This research's method determines the optimal areas in which to deploy SCMs to control runoff in urban catchments. The optimization method relies on a three-objective simulation-optimization model that (1) minimizes the volume of runoff at the catchment outlet and at flooding nodes, (2) minimizes the implementation and maintenance costs of LID SCMs, and (3) minimizes the service-performance reduction of LID SCMs. The storm water management model (SWMM) is applied for runoff simulation and is coupled with the multi-objective antlion optimization algorithm (MOALOA). The simulation-optimization method is exemplified with an application to District 6 of Tehran's municipality (Iran). The performance of the simulation-optimization method is compared with that of the multi-objective non-dominated sorting genetic algorithm II (NSGAII), and, after confirming the superior capacity of the MOALOA, the latter algorithm is applied to District 6 of Tehran municipality, Iran. The identified optimal LID SCMs are ranked with the technique for order of preference by similarity to ideal solution (TOPSIS) method that reveals the preferences of the runoff managers concerning SCMs choices. The most desirable solution herein found shows the optimal LID SCMs provide a significant reduction in runoff volume at the catchment outlet and flooding nodes.

Key words | antlion optimization algorithm, low-impact development practices, multi-criteria decision-making, optimization, simulation, stormwater management

Melika Mani
Omid Bozorg-Haddad (corresponding author)
Department of Irrigation and Reclamation
   Engineering, Faculty of Agricultural Engineering
   and Technology, College of Agriculture and
   Natural Resources,
University of Tehran,
Karaj, Tehran,
Iran
E-mail: obhaddad@ut.ac.ir

Hugo A. Loáiciga
Department of Geography,
University of California,
Santa Barbara, CA 93016-4060,
USA

INTRODUCTION

Increased urbanization and the replacement of pervious or semi-pervious surfaces with impervious surfaces has been a key factor causing more runoff from precipitation in urban areas (Davis 2005), which increases peak flows and reduces the time to peak flow (Holman-Dodds et al. 2003). Urban runoff carries various pollutants from urban areas into the receiving waters (Davis et al. 2009; Barkdoll et al. 2016). Studies show that in highly urbanized areas, the volume of runoff generation is significant (Xu & Zhao 2016; Yao et al. 2018); moreover, as a result of intensifying extreme rainfall events flood risk increases (Hettiarachchi et al. 2018). Therefore, appropriate management of urban runoff with low-impact development (LID) stormwater control measures (SCMs) is currently a preferred approach to urban runoff management (Sadeghi et al. 2017).

LID SCMs constitute an approach to stormwater management that emphasize the use of small scale, water-retaining features within urban areas to slow, purify, infiltrate and capture urban runoff and precipitation at the point of origin (Davis 2005; Chau 2009; Morsy et al. 2016).

www.manaraa.com

There are several types of LID SCMs with varying installation and maintenance costs. Bioretention cells, vegetated swales, rain gardens, porous pavements, dry (infiltration) wells, and infiltration trenches are the most common LID SCMs. They exhibit variable performance in runoff infiltration, detention, and removal of pollutants. Various studies of LID SCMs have been conducted to evaluate their performance in terms of quantitative and qualitative control of urban runoff, such as those dealing with bioretention cells (Davis 2008; Dietz & Clausen 2008; Hunt et al. 2008; Carpenter & Hallam 2009; James & Dymond 2011; Lucke & Nichols 2015; York et al. 2015), on porous pavement (Collins et al. 2009; Fassman & Blackbourn 2010; Brunetti et al. 2016; Huang et al. 2016; Alsubih et al. 2017; Kamali et al. 2017), and infiltration trenches (Emerson et al. 2010) and on vegetated swale (Fach et al. 2011).

Successful and economical application of LID SCMs requires careful selection, design, and the area over which they are deployed. An effective approach to SCM selection, sizing, and deployment is to combine runoff simulation with optimization of SCMs. In many applications there are many sub-catchments within a catchment, complicating the choice of the most effective layout of candidate LID SCMs without resorting to optimization approaches (Cano & Barkdoll 2016; Eckart et al. 2018). Several authors have addressed the problem of SCMs selection, layout, and design with quantitative, qualitative, and economic criteria by applying the simulation-optimization approach. In some studies, minimizing runoff volume or runoff peak flow and LID SCMs costs (quantitative and economic criteria) were considered (Jia et al. 2012; Damodaram & Zechman 2012; Tao et al. 2014; Eckart 2015; Loáiciga et al. 2015; Chui et al. 2016; Aminjavaheri & Nazif 2018). Other studies considered the objectives of minimizing runoff pollution and LID SCMs costs (qualitative and economic criteria) (Baek et al. 2015; Tobio et al. 2015). Several authors combined quantitative, qualitative and economical criteria in the selection, sizing, and location of SCMs for runoff control (Limbrunner et al. 2013; Montaseri et al. 2015; Sadeghi et al. 2017). The cited studies assumed temporal constant performance for each LID SCM neglecting the effect of clogging on their performance over time.

LID SCMs are impaired by clogging due to sedimentation of suspended solids or by the accumulation of oil and grease, blockage by accumulated trash, or by reduction of their infiltration and filtration capacities by biological growth. LID SCMs performance declines over time despite periodic maintenance (Haselbach et al. 2016) until replacement takes place. Many experimental, field, and theoretical studies have been conducted to assess clogging effects on LID SCMs and their long term performance (Haselbach et al. 2006; Lucke & Beecham 2011). These studies determined the effect of clogging as the ratio of the permeability reduction to the permeability in the unclogged state (Deo et al. 2010; Freni & Mannina 2018), as a percentage of the long term hydraulic conductivity reduction (Li & Davis 2008; Pezzaniti et al. 2009), or as an analytical probabilistic expression (Zhang & Guo 2014). The reduction of LID SCMs service performance over time varies among LID SCMs depending on site-specific features.

This paper presents a multi-objective simulation-optimization model to determine optimal combination of LID SCMs in urban areas. The model includes economic and quantitative criteria, and considers the reduction of LID SCMs service performance over time. The consideration of service-performance reduction of LID SCMs has been rarely accounted for in previous studies. The simulation-optimization model links the SWMM simulation model to the multi-objective antlion optimization algorithm (MOALOA) by coding them in MATLAB2012b considering three-objective goals: (1) minimizing the runoff volume at the catchment outlet and the overflow volume at nodes to increase urban drainage system reliability that reduces flood potential, (2) minimizing the cost of implementation and maintenance of LID SCMs, and (3) minimizing the service-performance reduction of LID SCMs by choosing efficient SCMs layout. The solutions of the multi-objective optimization of SCMs are expressed in terms of Pareto possibility frontiers, or Pareto fronts, that represent alternative optimal combinations of SCMs with inherent tradeoffs among objectives. The TOPSIS method (Hwang & Yoon 1981) is implemented for selecting the most desirable LID SCMs solution according to weighting criteria.

MATERIALS AND METHODS

The outline of this work is as follows:

1. Choosing a simulation model and optimization algorithm.

2. The simulation-optimization model is developed by coupling the simulation model to the optimization algorithm.

3. The performance of the optimization algorithm is evaluated by means of an example problem from the SWMM manual.

4. The simulation model is built for the study area (District 6 of Tehran municipality).

5. The design rainfall hyetograph is developed and applied to the simulation model.

6. The catchment's stormwater infrastructure is evaluated.

7. Suitable LID SCMs are selected for the study area conditions and from results of previous studies.

8. The simulation-optimization model is implemented and optimal management alternatives are determined.

9. The most desirable solution is selected among those on the optimal Pareto front using the TOPSIS method.

The next section explains the methodology in detail.

Rainfall-runoff simulation model for the study area

The SWMM is implemented as the rainfall-runoff model. Afterwards, appropriate LID SCMs are identified for improving the study area's drainage system performance.

The SWMM

Among the simulation models, the US Environmental Protection Agency (USEPA) storm water management model (SWMM) has been widely used for qualitative and quantitative simulation of runoff in urban areas and LID SCMs. Jayasooriya & Ng (2014) evaluated and compared 20 models for urban runoff management. They singled out SWMM developed by the United States environmental protection agency (USEPA) as one of the most accurate and practical models.

The site or catchment simulated with SWMM is divided into subcatchments. Subcatchments receive precipitation and generate runoff and pollutant loads. Runoff and pollution loads are routed through channels and pipes to the outlet of the catchment (Rossman 2015).

LID SCMs simulation

SWMM 5.1 contains a toolbox to model common types of LID SCMs explicitly and computes the absorption and retention of runoff and pollutants. There are several LID SCMs that are chosen based on site features such as land use, terrain slope, environmental characteristics, and precipitation regime. This study considers several LID SCMs described in the SWMM's user manual. The LID SCMs considered for deployment in the main case study (District 6 of Tehran municipality) are porous pavement and bioretention cells. Advantages of porous pavement are its capacity to reduce the volume of runoff and peak flow (Fassman & Blackbourn 2010; Palla & Gnecco 2015; Alsubih et al. 2017). Moreover, it is ideal for sites with limited space for other LID SCMs, making it a good choice for highly urbanized environments. Previous studies have shown considerable reduction of runoff volume and peak flow by bioretention cells (Dietz 2007; Line & Hunt 2009; Trinh & Chui 2013; Eckart et al. 2017). Bioretention cells are suitable for implementing alongside streets and on parking lots to control runoff and provide natural green spaces.

The parameters of LID SCMs are determined and defined in the SWMM according to site conditions (District 6 of Tehran municipality) as reported in previous studies (PaDEP 2006; Fallahi Zarandi 2013; Eckart 2015; Chui et al. 2016) and the SWMM users' manual (Rossman 2015). The parameter values are listed in Table 1. The soil characteristics are nearly constant in the study area; therefore, similar LID SCMs were considered in all the subcatchments. The maximum percentage of clogging or blockage in porous pavement, bioretention cells, vegetated swales, and infiltration trenches were set equal to 40%, 20%, 20%, and 30%, respectively. These values were assigned considering each LID SCMs performance in previous laboratory studies and field studies in similar study areas (Siriwardene et al. 2007; Li & Davis 2008; Pezzaniti et al. 2009; Deo et al. 2010; Lucke & Beecham 2011; Razzaghmanesh & Becham 2018). The drainage area for each LID SCMs in each subcatchment was estimated based on land use maps. Pedestrian areas, low volume roads, and parking areas for implementing porous pavement, and alongside streets and

Table 1 | Design parameters of LID SCMs

	Parameter	Bioretention cells	Porous pavement	Vegetated swale	Infiltration trench
Surface	Berm height (mm)	150	4	200	100
	Vegetation volume fraction (%)	0.90	0	0.90	0
	Surface roughness coefficient	0.03	0.01	0.03	0.11
	Surface slope (%)	0	According to subcatchment slope	According to subcatchment slope	
Soil	Thickness (mm)	900	–	–	–
	Porosity (%)	0.50	–	–	–
	Hydraulic conductivity (mm/h)	250	–	–	–
Pavement	Thickness (mm)	–	100	–	–
	Void ratio	–	0.15	–	–
	Impervious surface fraction (%)	–	According to subcatchment impervious surface fraction	–	–
	Permeability (mm/h)	–	500	–	–
Storage	Thickness (mm)	500	350	–	700
	Void ratio	0.70	0.50	–	0.7
	Seepage rate (mm/h)	44	44	–	44

parking lots were taken into account in relation to bioretention cells.

Optimization

The decision variables of the optimization problem are the areas of LID SCMs in each subcatchment. The decision variables are expressed as follows:

$$DV = x_{ij} \quad i = 1, 2, 3, \ldots, n_s \quad j = 1, 2, 3, 4 \tag{1}$$

where DV = vector of decision variables, x_{ij} = area of LID SCM number j in subcatchment i, n_s = number of subcatchments, j represents the type of LID SCMs 1 = porous pavement, 2 = bioretention cells, 3 = infiltration trench and 4 = vegetated swale (only LID SCMs number 1 and 2 were considered in case study 2).

The decision variables are embedded in the simulation model linked to the optimization algorithm. Equations (2)–(4) express respectively objective functions 1, 2, and 3.

Objective function 1: reduction of the runoff volume at the catchment outlet and at flooding nodes:

$$Min \ Z_1 = 0.5 \times \left(\frac{VO_1 - VO_{min}}{VO_{max} - VO_{min}} \right) + 0.5 \times \left(\frac{FV_1 - FV_{min}}{FV_{max} - FV_{min}} \right) \tag{2}$$

where Z_1 = objective function 1, VO_1 = the volume of runoff at the outlet for normal operation when clogging and failure of LID SCMs do not occur, VO_{min} = the minimum runoff at the outlet when LID SCMs cover the maximum allowable area, VO_{max} = the maximum volume of runoff at the outlet when ID SCMs are not deployed, FV_1 = sum of overflow volume at all flooding nodes and for normal situation when clogging and failure of LID SCMs do not occur, FV_{min} = the sum of minimum flood volume at all flooding nodes when LID SCMs cover the maximum allowable area, FV_{max} = the sum of maximum overflow volume at all flooding nodes when LID SCMs are not deployed. The first term on the left-hand side of objective function (1) quantifies reduction of runoff volume at the outlet, while the second term quantifies decreasing flood potential at nodes where drainage system does not have sufficient capacity to pass the design runoff and overflows. Z_1 equals zero when all LID SCMs cover their maximum allowable areas, and Z1 becomes 1 when LID SCMs are not deployed. Considering FV and VO is necessary to prevent flooding inside and downstream the catchment respectively. Reducing the amount of runoff at the outlet of the catchment prevents flooding downstream the catchment which is a vulnerable urban area. This consideration is necessary in this study for reducing runoff overflow at flooding nodes inside the catchment.

Objective function 2: minimization of the SCMs construction and maintenance cost:

$$Min\ Z_2 = \sum_{j=1}^{J} \sum_{l=1}^{L} \frac{X_l(j) \times UC_l}{Maximum\ Cost} \tag{3}$$

where Z_2 = objective function 2, J = the number of subcatchments, L = the number of LID SCM types, $X_l(j)$ = the area of the lth LID SCM in the jth subcatchment, UC_1 = the unit cost of the lth LID SCM type, *Maximum Cost* = the cost of construction and maintenance of all LID SCMs covering the maximum allowable area.

Objective function 3: minimization of performance reduction of LID SCMs:

$$Min\ Z_3 = 0.5 \times \left(\frac{VO_2 - VO_1}{VO_1} \right) + 0.5 \times \left(\frac{FV_2 - FV_1}{FV_1} \right) \tag{4}$$

where Z_3 = objective function 3, VO_1 and VO_2 are defined identically as in Equation (1), VO_2 = the volume of runoff at the outlet when LID SCMs undergo maximum clogging and or blockage, and VF_2 = the sum of runoff volume at flooding nodes when LID SCMs undergo maximum expected clogging or blockage.

Concerning the second terms of objective functions 1 and 3 notice that if there are no flooding nodes in the study area then the runoff peak flow in the catchment outlet is considered instead of the sum of overflow volume at flooding nodes (FV) for the purpose of reducing the risk of downstream flooding.

The multi-objective antlion optimization algorithm

The antlion optimization algorithm (ALOA) and multi-objective version of the algorithm was introduced by Mirjalili (2015) and Mirjalili *et al.* (2017). It is inspired by the antlion hunting behavior at the larva stage. Mirjalili *et al.* (2017) applied the MOALOA for solving engineering problems and compared the MOALOA performance solving test mathematical functions with that of the particle swarm optimization (PSO) algorithms and the non-dominated sorting genetic algorithm (NSGAII). The MOALOA is implemented in the present study because of its relative superior performance in those comparative studies. The

performance of MOALOA in the simulation-optimization model of the present study is first evaluated with the optimization of the example runoff problem found in the SWMM application manual (Gironás *et al.* 2015).

The ALOA and MOALOA apply ants (i.e., the solutions) as search agents; the ants move over the decision space. Antlions (also the solutions because each ant has an antlion counterpart) combat and hunt the ants making the latter become fitter. The position of each ant is updated in each algorithmic iteration. The roulette wheel selection operator selects solutions (ants, antlions) with better fitness-function values (Pencheva *et al.* 2009; Mirjalili 2015). Table 2 lists the characteristics of the ALOA and MOALOA. The MOALOA and ALOA algorithms initialize the position of antlions and ants randomly, and calculates their fitness-function values, thus determining the elite ants and antlions. The roulette wheel operator selects one antlion for each ant in each iteration. Each ant's fitness function value is calculated: if an ant becomes fitter than its corresponding antlion its position becomes the new position of its antlion in the next iteration. The positions of ants are updated according to random walk (Mani *et al.* 2018).

The general framework of population-based evolutionary algorithms is similar (Bozorg-Haddad *et al.* 2017). The algorithms start the optimization process with generated populations of solutions which are compared with each other (Sarzaeim *et al.* 2018). The non-dominated solutions remain in the search algorithm. The evolutionary algorithms attempt to improve remaining solutions in the next iteration. What

Table 2 │ The characteristics of the MOALOA and ALOA (Mani *et al.* 2018)

General algorithm	Antlion optimizer
Decision variable	Antlion's and ant's position in each dimension
Solution	Antlion's position
Old solution	Old position of antlion
New solution	New position of antlion
Best solution	Elite antlion
Fitness function	Desirability of elite
Initial solution	Random antlion
Selection	Roulette wheel
The process of generating new solution	Random walk over the decision space

makes evolutionary algorithms different from one another is the method applied to enhance the non-dominated solutions.

Multi-objective optimization considers diversity and convergence in the improvement of the non-dominated solutions (Mirjalili *et al.* 2017). There are different methods for enhancing convergence such as archive and leaders, the non-dominated sorting mechanism, and niching. The MOALOA applies the archive-and-leaders approach to ensure suitable coverage.

Selecting an option from a set of alternative optimal solutions

Multi-criteria decision-making (MCDM) methods are implemented to select an option among several suitable alternative choices or solutions. The result of multi-objective optimization algorithms are expressed as a set of non-dominated solutions that form a Pareto possibility frontier or Pareto front. The technique for order of preference by similarity to ideal solution (TOPSIS) is a leading MCDM method used in water resources systems, and it was chosen here for selecting a most desirable solution among several alternative optimal solutions.

The TOPSIS method

The TOPSIS method attempts to prioritize management choices on the basis of proximity to the ideal choice and distance from the anti-ideal choice. TOPSIS takes into consideration the weights of criteria and the values of ideal and anti-ideal solutions of an optimization problem and ranks the solutions on the basis of their relative Euclidean distance from the ideal and anti-ideal solutions. TOPSIS identifies the solution closest to the ideal solution and farthest from the anti-ideal solution as the superior solution (Azarnivand & Banihabib 2016). The ideal solution is the most desirable to the decision-maker. Each optimization objective may have a separate ideal solution. The closer a solution is to the ideal value, the more desirable to the decision-maker. The anti-ideal solution is the worst solution for the decision-maker, and the decision-maker invariably prefers the solution obtained to be far from the anti-ideal solution (Banihabib *et al.* 2015; Bozorg-Haddad *et al.* 2016).

The steps of implementation of the TOPSIS method are as follows (Inanlu *et al.* 2012):

1. Constructing a decision matrix whose rows and columns represent criteria and choices (or solutions) that receive a quantitative value.
2. Normalizing the metrical elements' values to construct a normalized data matrix.
3. Determining the weight of each criteria and computing the weighted values for each matrix element through Equation (5):

$$F_{ij} = \pi_{ij} \times w_i \tag{5}$$

where F_{ij} = the weighted value of the ith row (criterion) and j^{th} column (choices or solutions) of the decision matrix, π_{ij} = the normalized value of the ith row and j^{th} column of the decision matrix, and w_i = the ith criterion weight.

4. Determining the ideal [A^+, Equation (6)] and anti-ideal [A^-, Equation (7)] solutions; this is done by the decision-maker.

$$A^+ = \{F_1^+, F_2^+, \ldots F_n^+\} \tag{6}$$

$$A^- = \{F_1^-, F_2^-, \ldots F_n^-\} \tag{7}$$

in which F_i^+, F_i^- represent ideal and anti-ideal decision variables, respectively, with $k = 1, 2, \ldots, n$.

5. Computing the Euclidean distance of the *j*-th solution from the ideal and anti-ideal solutions with Equations (8) and (9), respectively:

$$d_{j^+} = \sqrt{\sum_{i=1}^{n} (F_{ij} - F_i^+)^2} \tag{8}$$

$$d_{j^-} = \sqrt{\sum_{i=1}^{n} (F_{ij} - F_i^-)^2} \tag{9}$$

d_{j^+} and d_{j^-} denote the Euclidean distances from the *j*-th solution to the ideal and anti-ideal solutions, respectively.

6. Computing the proximity of the *j*-th solution to the anti-ideal solution, defined as follows:

$$Cl_j = \frac{d_{j^-}}{(d_{j^-} + d_{j^+})} \text{ for all j} \tag{10}$$

7. Ranking the solutions on the basis of the value of CL_i such that the closer this amount is to zero, the lower the rank; and the closer it is to 1, the higher the rank.

The decision-making must choose from the set of optimal solutions of the multi-objective optimization problem, each of which is superior to others at least in terms of one objective. This study applies the TOPSIS method with equal weights to the three-objective functions to choose a most desirable solution among those present in the MOALOA-calculated Pareto front of solutions.

CASE STUDIES

Two case studies are solved in this work. The first is the example appearing in the application manual of the SWMM. The solutions calculated with the MOALOA are compared with those of the NSGAII to serve as a test of the MOALOA relative to the well-established NSGAII.

The second case study deals with District 6 of Tehran municipality. This district is predominantly residential with predominant impervious surface, which causes flooding during heavy rains. MahabGhods Consulting Engineering Company (2011a, 2011b) recommended the use of LID SCMs in all areas of the city of Tehran.

Sample case of the SWMM application manual

The SWMM's example is a catchment of 117,359 m^2 divided into seven subcatchments. The areas of the subcatchments range between 8012 and 27,478 m^2, and their slopes range between 2% and 3%. The fraction of impervious areas in the subcatchments varies between 0% and 40%. The input data including the design rainfalls with return periods of 2, 5, and 10 years and subcatchments' features are found in the SWMM manual (Gironás *et al.* 2015). Here the SWMM is implemented with a 2-hour design rainfall with a 10-year return period, in which 43.45 mm of rainfall occurred within 2 hours.

District 6 of Tehran municipality

District 6 of Tehran municipality has an area equal to 2,137.18 hectares (1 ha = 10^4 m^2), and is in central Tehran. This is a highly urbanized site including residential areas, streets, parks, and the University of Tehran. It is shown in Figure 3 that District 6 is divided into 45 subcatchments

(Tehran University-Graduate Faculty of Environment 2015). The slope of the subcatchments varies between 1% and 4%, and the impervious fraction near 100% in most of the subcatchments and declining to 30–40% in a few subcatchments where there are parks with pervious surfaces. The drainage system of this area includes 30 circular buried channels with 1.6-meter depth, and one rectangular open channel with 0.7-meter depth. The Manning roughness coefficient of channels are in the range of 0.012–0.035.

A study by the MahabGhods Consulting Engineering Company (2011a, 2011b) established a design storm with a duration of 6 hours and a return interval equal to 25 years for the study area. The same study concluded that the time of concentration for the entire city of Tehran equals 3 hours, implying that the District 6 concentration time is shorter. The 2011 study proposed the following rainfall intensity equation for the 25-year return period storm:

$$i = 237 \times D^{-0.645} \tag{11}$$

where i = rainfall intensity (mm/h) and D = rainfall duration (minutes).

Calculating costs of implementation and maintenance of LID SCMs

The expense for LID SCMs includes all costs of their construction and maintenance during their 20-year service life. It is determined based on the list of values issued by the Management and Planning Organization of Iran (2017) and the study by Fallahi Zarandi (2013). The costs from the study by Fallahi Zarandi are scaled to 2017 costs by applying the cost-appreciation rate applicable in Iran (Central Bank of the Islamic Republic of Iran 2017).

The annual cost of repair and maintenance for porous pavements, bioretention cells, infiltration trenches and vegetated swales equal 10%, 5%, 6% and 3% of their construction costs (PaDEP 2006; Fallahi Zarandi 2013; Osouli *et al.* 2017). Equation (12) converts these costs to current value:

$$C = A \times \left[\frac{(1+i)^N - 1}{i \times (1+i)^N} \right] \tag{12}$$

where C = current equivalent cost, A = annual cost, N represents the service life of LID SCMs, in years.

RESULTS

Evaluating the performance of the SWMM-MOALOA simulation-optimization model with a SWMM sample problem

The relative superior performance of the MOALOA compared with the NSGAII and the multi-objective particle swarm optimization (MOPSO) algorithm has been demonstrated with several optimization problems (Mirjalili 2015; Mirjalili *et al.* 2017). The SWMM was linked with the MOALOA and with the NSGAII in MATLAB Version 2012. The SWWM manual's sample problem was solved with the two simulation-optimization models. The simulation-optimization model was run 10 times with the MOALOA-SWWM and the NSGAII-SWWM under identical conditions using a Core i7 computer with a processing speed of 3.5 GHz and a memory of 8 GB. The sample catchment is divided into seven subcatchments (Gironás *et al.* 2015), one of which is 100% pervious and does not require runoff control. Four LID SCMs were considered for deployment, namely, porous pavement, bioretention cells, infiltration trench, and vegetated swales, in the six remaining subcatchments. This means there are 24 decision variables to be optimized. These decision variables are the areas over which each LID SCM would be constructed within each subcatchment. The unit costs of implementation and maintenance for porous pavement, bioretention cells, vegetated swales, and infiltration trench were set equal to $10, $19.75, $7.64, and $16.15, respectively. The objective functions defined for this sample problem are those expressed by Equations (2)–(4), except that the parameter FV (the sum of overflow volume at flooding nodes) is replaced by the peak flow at the outlet in Equations (2) and (4). There are no flooding nodes in this example; therefore, peak flow was deemed the appropriate variable to simulate in this example to reduce the risk of downstream flooding. This problem was solved using MOALOA-SWMM and NSGAII-SWMM with 100 iterations and 50 prospective solutions in the initial population of solutions. Figure 1 illustrates the Pareto front resulting from the combination of the 10 runs of each algorithm.

As seen in Figure 1(a), the solutions of the Pareto front from 10 runs of the MOALOA-SWMM (whose calculated
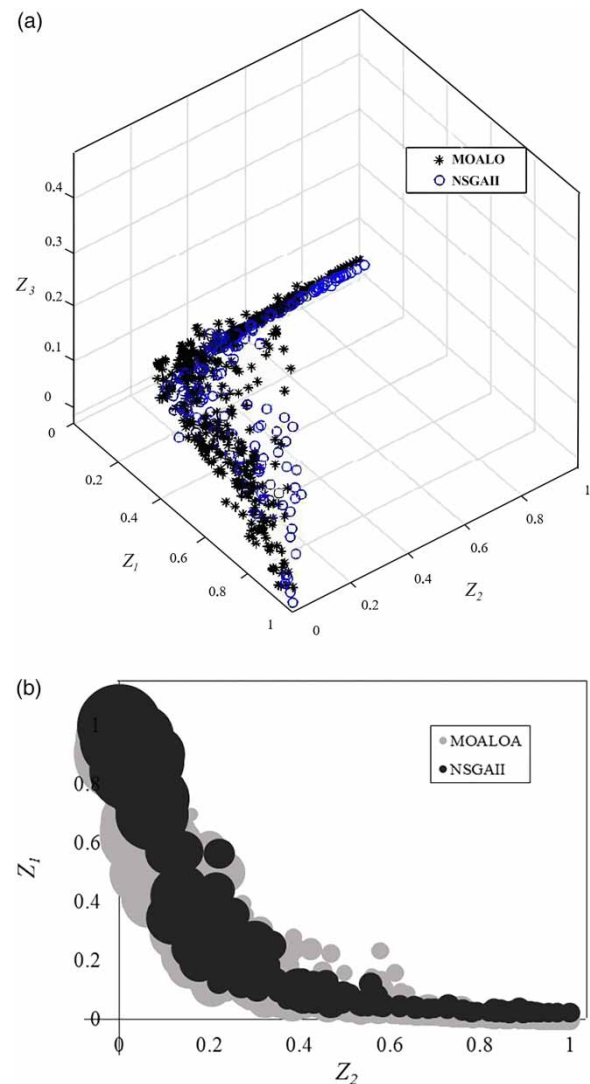
Figure 1 | Pareto fronts calculated with the MOALOA-SWMM and NSGAII models: (a) three-dimensional representation; (b) two-dimensional representation. The diameters of the circles represent the value of the third objective function.

solution are markers shaped as stars) have a closer distance to the origin of coordinate than the NSGAII-SWMM solutions, thus the former solutions are closer to the ideal solution. Table 3 lists various features of the simulation-optimization runs. As seen in Table 3 the average Euclidean distances of the MOALOA-SWMM Pareto fronts (recall there were 10 runs) from the origin of coordinate vary between 0.4 and 0.62, while those of the NSGAII-SWMM vary between 0.53 and 0.69. Evidently the Euclidean distances of the best and the worst runs of MOALOA-SWMM are 0.13 and 0.07 less (better) than the corresponding

www.manaraa.com

Table 3 | Features of 10 runs of the MOALOA and NSGAII

Algorithm	Feature	Run 1	Run 2	Run 3	Run 4	Run 5	Run 6	Run 7	Run 8	Run 9	Run 10
MOALOA	Mean Euclidean distance between Pareto front and the origin of the coordinate system	0.40	0.61	0.58	0.62	0.53	0.57	0.50	0.47	0.45	0.51
	Number of points on the Pareto front	100	93	94	92	98	89	92	100	100	86
	Run Time (s)	2,950	2,743	2,695	2,849	2,615	2,754	2,917	2,825	2,990	2,890
	Hyper Volume indicator for objective functions (1) and (2)	0.2	0.28	0.25	0.29	0.26	0.28	0.24	0.23	0.22	0.26
	Hyper Volume indicator for objective functions (2) and (3)	0.1	0.13	0.13	0.12	0.11	0.11	0.12	0.1	0.11	0.12
NSGAII	Mean Euclidean distance between Pareto front and the origin of the coordinate system	0.57	0.53	0.58	0.69	0.58	0.61	0.59	0.60	0.60	0.60
	Number of points on the Pareto front	20	18	18	18	18	16	20	18	15	15
	Run Time (s)	2,985	2,864	2,689	2,762	2,889	2,850	2,828	2,735	2,963	2,912
	Hyper Volume indicator for objective functions (1) and (2)	0.28	0.25	0.26	0.3	0.28	0.28	0.28	0.27	0.28	0.28
	Hyper Volume indicator for objective functions (2) and (3)	0.1	0.1	0.11	0.13	0.1	0.13	0.11	0.13	0.11	0.12

values of NSGAII-SWMM, respectively, and the Pareto front resulting from the best run of the MOALOA-SWMM is approximately 1.72 times nearer the coordinate's origin than the best Pareto front calculated with the NSGAII-SWMM. The hyper volume index for objective functions 1 and 2, and objective functions 2 and 3 was calculated considering (0,0) as the base point. The average hyper volume values of objective functions 1 and 2 for 10 runs equal 0.251 and 0.276 respectively for MOALOA and NSGA II. The average hyper volume values of objective functions 2 and 3 equal 0.115 and 0.114 respectively for MOALOA and NSGA II. The results show overall better performance of the MOALOA-SWMM.

Figure 1(b) depicts a two-dimensional view of the Pareto fronts calculated with the MOALOA-SWMM and NSGAII-SWMM models. The value of the third objective function is represented in Figure 1(b) by the diameter of the circles chosen as markers to represent the calculated solutions. It is seen in Figure 1(b) that there are a few points on the MOALOA Pareto that are located above those of the NSGAII Pareto in relation to the x and y axes, yet the value of the third objective function is smaller (and thus preferable) for the MOALOA solutions.

The results from this SWWM sample problem demonstrate the capacity of the MOALOA-SWMM model when tested against the well-known NSGAII model coupled with the SWMM. The next sections describe the implementation of the MOALOA-SWMM model to the LID SCMs optimization in District 6 of Tehran.

The design hyetograph, and runoff generation in District 6 of Tehran municipality

The application of Equation (10) and the alternating block method produce the design hyetograph shown in Figure 2. The 25-year return period design hyetograph was developed based on the Tehran Stormwater Management Master Plan (MahabGhods Consulting Engineering Company 2011a, 2011b). The rainfall duration is longer than the concentration time because the largest peak runoff rate occurs when the entire drainage area is contributing (USDA SCS 1986). The SWWM simulated runoff associated with the design hyetograph in the absence of LID SCMs. The input parameters for SWMM such as curve number, urban percent of imperviousness, depression storage, and Manning's roughness coefficient were calibrated by Tehran University, Faculty of Environment (Tehran University-Graduate Faculty of environment 2015). The results show that runoff volume produced by the design rainfall exceeds the conduit capacity in the four nodes. Table 4 lists the duration, discharge, and volume of overflow at four flooding nodes. Figure 3 depicts the locations of flooding nodes within the study catchment. The runoff volume and peak
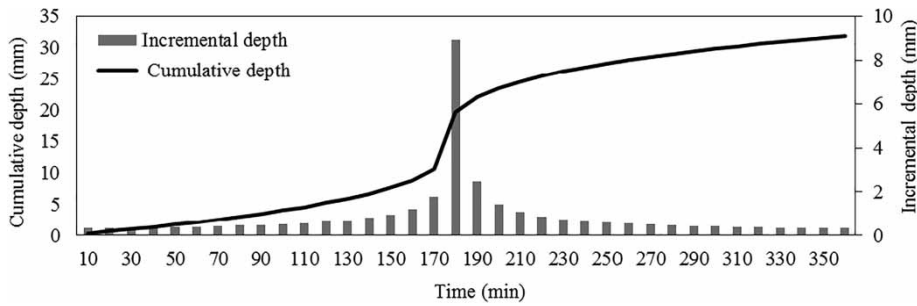
Figure 2 | Hyetograph and cumulative depth of 6-hour, 25-year design rainfall for the study area developed with the alternating block method.
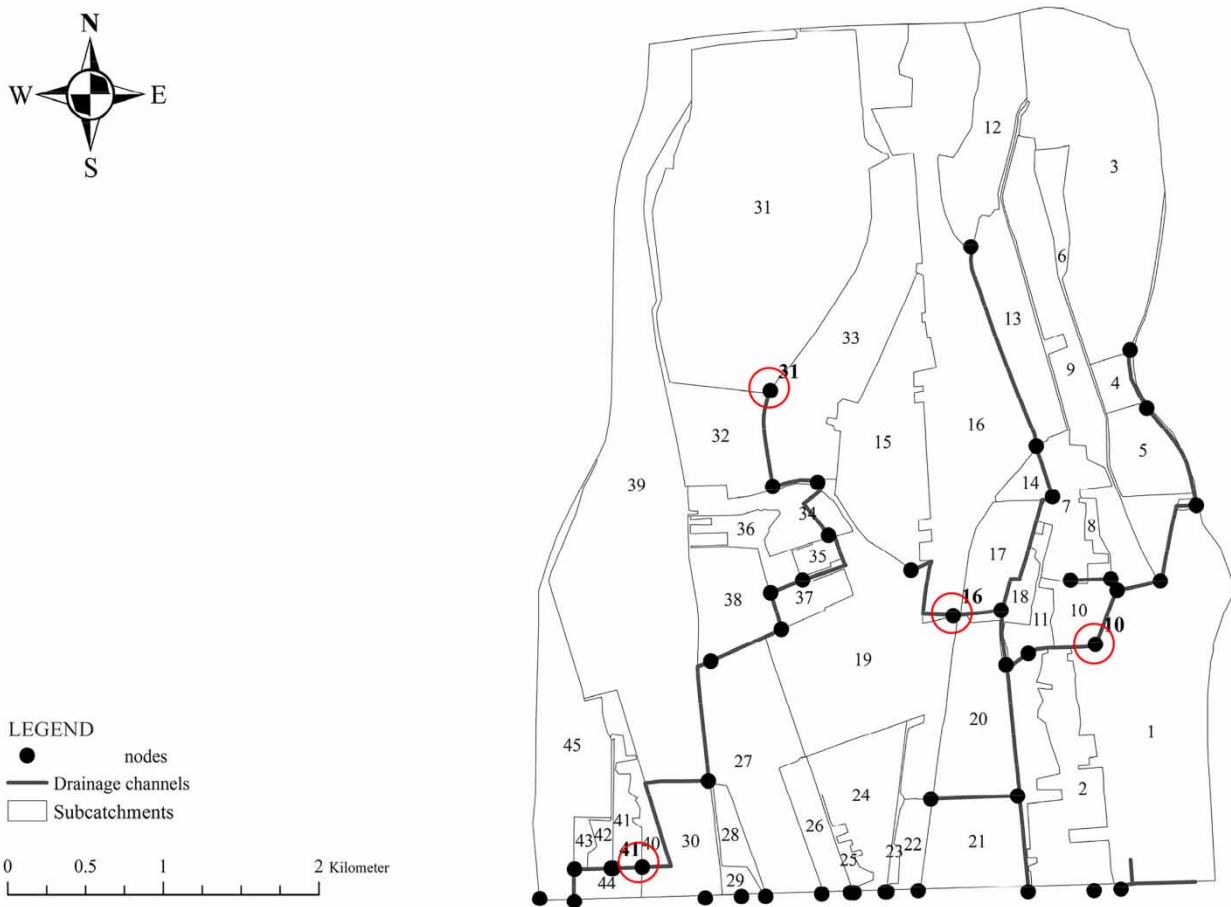

Figure 3 | The locations of flooding nodes in District 6 of Tehran municipality.

flow at the site outlet equal $581.05 \times 10^3 \, \text{m}^3$ and $71.66 \times 10^3 \, \text{m}^3/\text{s}$, respectively. These runoff volumes and peak flows at the catchment outlet and flooding nodes inside the catchment may induce flooding in the downstream urban area and within the catchment. Therefore, LID SCMs are deployed to improve the performance of the drainage system and decrease the risk of downstream flooding.

Table 4 | Flooding nodes data

Node no.	Duration (h)	Maximum overflow discharge (m³/s)	Total overflow volume (m³10³)
10	0.69	5.01	6.55
16	3.41	7.57	30.64
31	2.74	11.70	33.40
41	0.26	1.70	1.07

Results from the NSGAII-SWMM and MOALOA-SWMM for LID SCMs optimization in District 6 of Tehran

The three-objective problem of the present study was solved with MOALOA and NSGAII applying 100 iterations and an initial population size of 150 solutions. The number of decision variables equals 90 (=45 subcatchments × 2 possible SCMs per subcatchment). The decision variables represent the areas over which a type of LID SCM is deployed within each subcatchment.

Figure 4(a) illustrates the Pareto fronts calculated with the MOALOA-SWMM and NSGAII-SWMM models in three dimensions. Figure 4(b) depicts the same results in a two-dimensional visualization. The diameters of the circles represent the value of the third objective function in Figure 4(b). The smaller diameters signify better solutions under minimization. It is seen in Figure 4(a) and 4(b) that the MOALOA-SWMM solutions have wider distribution (that is, greater diversity of choices or solutions) and greater density than the NSGAII-SWMM solutions. The MOALOA-SWMM model produces 135 non-dominated Pareto solutions compared with 50 by the NSGAII-SWMM model. Figure 4(b) shows that the NSGAII-SWMM model produced no solutions for $Z_1 < 0.1$, while MOALOA produced non-dominated solutions for objectives Z_1 and Z_2 for the entire defined feasible range of solutions. This demonstrates the capacity of the MOALOA-SWMM model to more precisely and broadly (diversity) search the multi-objective space of the optimization problem and calculate non-dominated Pareto solutions. It is worth noting that the average Euclidean distance from the origin of the coordinate system for the final Pareto front calculated with the MOALOA-SWMM equals 0.637, and that of the Pareto calculated with the NSGAII-SWMM model equaled 0.764. This indicates the Pareto front produced by MOALOA-SWMM is closer to the ideal solution (located at the origin of the coordinate system under minimization).

Figure 5 depicts the non-dominated Pareto solutions of the three-objective optimization. The numbers on the x-axis and the y-axis represent the values of the first objective function (minimization of the volume of runoff at the outlet of the catchment and at flooding nodes) and the second objective function (minimization of the construction and maintenance cost of LID SCMs), respectively. The
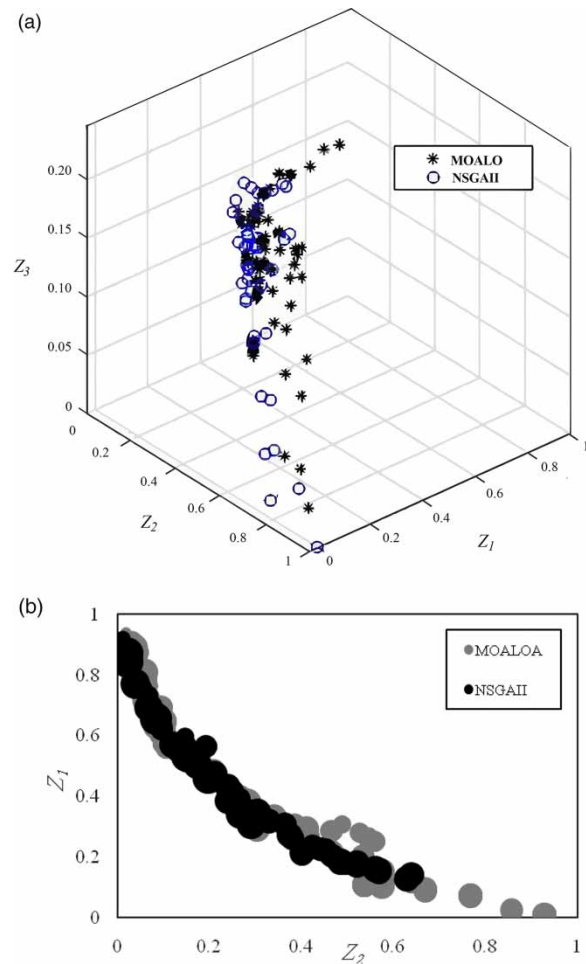
Figure 4 | The calculated Pareto fronts from the three-objective optimization of the study area (a) in three dimensions and (b) in two dimensions whereby the diameter of the circles expresses the magnitude of objective 3.

points or solutions on the Pareto front are represented by circles with different diameters, whose sizes denote the value of the third objective function (reduction of system performance due to failure of LID SCMs by clogging and blockage). The smaller diameters signify better solutions under minimization.

It is seen in Figure 5 that as the second objective function (which represents cost) increases (worsens) from 0 to 0.5, the first objective function decreases (improves) from 0.9 to about 0.15, and, thenceforth, the decreasing trend of the first objective function continues with a lower slope. In fact, as the second objective function increases from 0.5 to 0.9, the first objective function decreases by only 0.15. This indicates that marginal improvement of the first
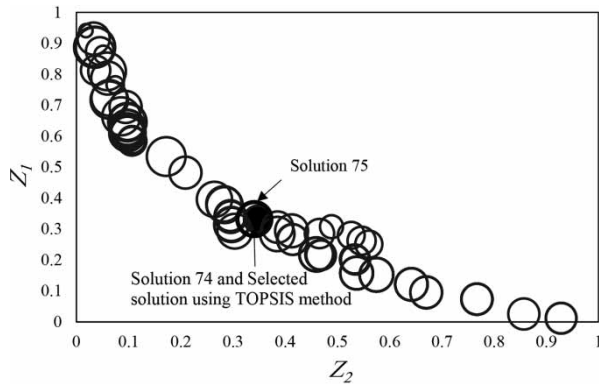
www.manaraa.com

Figure 5 │ The Pareto front resulting from three-objective optimization.

objective drastically decreases for Z2 > 0.5. Figure 5 shows that there are solutions with different diameters that signify the value of the third objective function (or reduction of LID SCMs performance) on the Pareto front.

The third objective function plays an important role in the selection of LID SCMs. This is so because for close values of the first and second objective function the magnitude of the difference between the values of the third objective function signifies the difference in reduction performance of the LID SCMs due to clogging and blockage. Table 5 lists the values of two solutions on the Pareto fronts with similar first and second objective functions. According to Table 5 for the two solutions numbered 74 and 75, signaled by arrows in Figure 6, the first and second objective functions have approximately equal values, but the third objective function has different values for these solutions, which indicates a difference in the reduction of service performance of the LID SCMs associated with each solution. After blockage and reduction of the performance of LID SCMs the volume of runoff at the outlet of the subcatchments and the volume of runoff at flooding nodes increased by 12.8 and 1.41 thousand cubic meters, respectively, for Solution 74, while they increased by 24.2 and 5.47 thousand cubic meters, respectively, for Solution 75. The runoff at the outlet is twice larger for

Solution 75 than that of Solution 74, and the runoff at the flooding nodes is five times larger for Solution 75 than that of Solution 74. This considerable difference in runoff underlines the importance of including the third objective function in selecting SCMs with better service performance, which is called service reliability. Otherwise Solutions 74 and 75 would be nearly indistinguishable from each other, yet, by including objective function 3 (reduction of performance) Solution 74 is clearly superior in the long run.

The MOALOA-SWMM model was run for District 6 of Tehran employing the first objective function (Equation (2)), reduction of the runoff volume at the catchment outlet and at flooding nodes, and the second objective function (Equation (3), minimization of the SCMs construction and maintenance cost). Figure 6 shows that the Pareto front generated by this two-objective optimization with MOALOA-SWMM has suitable density, coverage, and incorporates all the solutions from the highest to the lowest values of both objective functions, demonstrating the accurate and effective performance of the simulation-optimization model. These Pareto solutions reduce the volume of outlet runoff and the volume of runoff at flooding nodes between 0 and 215.8×10^3 m³ and between 0 and 51.243×10^3 m³ for a cost of 0 to \$47,932. The next section applies the TOPSIS method to select the most desirable solutions employing two-objective and three-objective optimization and compares the impact of considering objective 3
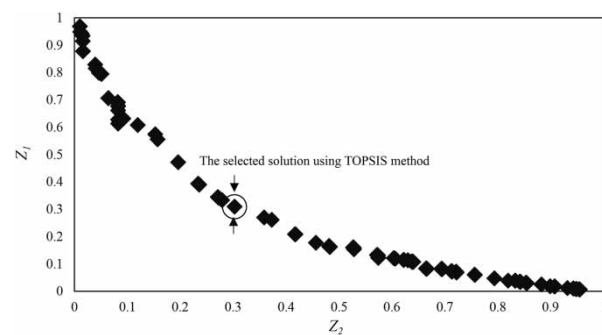

Figure 6 │ The Pareto front of two-objective optimization.

Table 5 │ Comparison of two points of the Pareto front

Solution point no.	Objective function 1	Objective function 2	Objective function 3	Difference between VO_2 and VO_1 (10^3 m³)	Difference between VF_2 and VF_1 (10^3 m³)
74	0.331	0.347	0.104	12.803	1.412
75	0.332	0.340	0.163	24.289	5.470

(reduction of LID SCMs performance over time) in the deployment of LID SCMs.

Determining the most desirable solutions with the TOPSIS method

Figures 5 and 6 show the most desirable solutions selected with the TOPSIS method corresponding to the three-objective and two-objective optimizations, respectively. The two-objective solution is such that the reductions of the volumes of runoff at the outlet and at the flooding nodes equal 163.4×10^3 and $43.24 \times 10^3\,\mathrm{m}^3$, respectively, for a cost of $\$18.54 \times 10^6$ of LID SCMs. By considering maximum blockage and the failure percentage of LID practices the amount of volume of runoff at outfall and the amount of runoff at flooding nodes are increased by 27.3×10^3 and $7.2 \times 10^3\,\mathrm{m}^3$, respectively, in comparison with the assumed condition in which clogging does not occur. The three-objective optimization solution produced reductions in the volumes of runoff at the outlet and at the flooding nodes equal to 121×10^3 and $32.69 \times 10^3\,\mathrm{m}^3$, respectively, with a cost of $\$14 \times 10^6$. By considering the maximum percentage of blockage and failure of LID SCMs practices runoff at the outlet and at flooding nodes increases by 12.8×10^3 and $1.41 \times 10^3\,\mathrm{m}^3$ respectively in comparison with the assumed condition in which clogging does not occur. This considerable reduction of runoff between the cases in which clogging of LID SCMs is assumed not to occur and that in which it does occur demonstrates the necessity of taking account of the third objective function, which improves the selection of LID SCMs by leading to greater service reliability.

TOPSIS method's most desirable solution associated with the three-objective optimization selected deployment of porous pavement in 34% of the maximum area that could be allocated to this LID SCM, which equals 808,135 m^2, and allocated bioretention cells over 35% of the maximum area that could be allocated to this LID SCM, which equals 300,878 m^2. Bioretention cells are costlier than porous pavement, yet, previous studies have demonstrated that they are less vulnerable to blockage and clogging (Li *et al.* 2009).

Table 6 lists the maximum allowable areas' percentages for implementing LID SCMs, and their optimal percentages of the total areas of subcatchments. The maximum possible

areas for implementing LID SCMs is determined based on land use maps of the study area. The optimal areas for LID SCMs in each subcatchment are the result of three-objective optimization, which are shown as the percentage of the total subcatchment areas as listed in Table 6 and Figure 7.

Figure 7 depicts the spatial distribution of the LID SCMs associated with the most desirable solution obtained with three-objective optimization (calculated percentage area of LID SCMs to their maximum allowable percentage area). It can be seen in Figure 7 the upstream subcatchment encompassing node 31 has a low-percentage area of LID SCMs because the cause of flooding at node 31 is runoff entering as inflow from an upstream catchment. Therefore, the deployment of LID SCMs in subcatchment of node 31 would not be effective. In contrast, the subcatchments with nodes 10 and 16 have large areas covered by LID SCMs. Evidently, the selected solution provides optimal LID SCMs based on their capacity to reduce runoff, their costs, and their service reliability, features that have a strong geographical context given the heterogeneity of land-use conditions. Generally, subcatchments in which runoff passes through the flooding nodes are more suitable for allocating LID SCMs and produce more effective designs.

Table 7 reports the runoff volume at flooding nodes before and after applying the LID SCMs. These values demonstrate the runoff volume at flooding nodes is reduced considerably. Yet, at node 31 the runoff volume is only slightly reduced because it enters as inflow from upstream areas. Table 8 lists the peak discharge, the runoff volume, and the time to peak discharge at the catchment outlet before and after LID SCMs deployment. It is evident from Table 8 that LID SCMs reduce the runoff volume by 121,000 m^3 and delays the time to peak discharge by 20 minutes. Figure 8 depicts the outflow hydrograph before and after applying LID SCM. It is evident from Figure 8 the reduction of the peak discharge and the delay in the time to peak discharge.

CONCLUSION AND DISCUSSION

The transition of native landscapes to urban areas increase the impervious surfaces. These changes reduced infiltration, which leads to increased runoff and flood risks in urban areas. LID SCMs are deployed to decrease the stress on urban stormwater infrastructure, improve their performance,

Table 6 | Percentage of LID SCMs in each subcatchment

Subcatchment	Maximum possible area / Total area %		Optimum area / Total area %	
	Porous pavement	Bioretention cells	Porous pavement	Bioretention cells
1	11	5	5.7	1.6
2	11	6	4.9	1.3
3	10	5	3.4	1.7
4	11	5	0.5	1.9
5	12	4	4.3	1.8
6	9	5	2.7	1.9
7	11	5	2.6	2.1
8	12	4	6.1	2.3
9	11	5	1.6	2.0
10	8	6	2.9	1.9
11	12	4	4.7	1.9
12	10	6	3.0	1.7
13	11	5	3.0	0.4
14	14	5	6.4	2.5
15	12	5	4.5	1.0
16	10	5	6.0	1.4
17	11	5	3.7	1.7
18	10	7	7.6	0.5
19	10	7	5.0	1.6
20	12	6	3.7	0.3
21	10	5	3.2	1.2
22	15	7	3.0	0.7
23	11	6	2.0	1.4
24	11	5	2.3	2.1
25	11	5	1.0	2.2
26	11	5	4.9	0.9
27	9	5	3.8	1.8
28	8	4	1.2	2.0
29	12	5	4.6	0.3
30	11	5	5.5	0.1
31	11	6	0.1	1.0
32	12	3	1.6	0.3
33	13	7	3.2	0.7
34	10	6	2.9	1.8
35	11	7	4.6	1.6
36	11	6	7.3	2.3
37	11	6	0.3	1.8
38	12	5	6.0	1.7

(*continued*)

Table 6 | continued

Subcatchment	Maximum possible area / Total area %		Optimum area / Total area %	
	Porous pavement	Bioretention cells	Porous pavement	Bioretention cells
39	11	5	5.9	2.1
40	10	6	5.1	1.5
41	10	8	1.7	1.6
42	10	6	5.4	0.3
43	11	5	4.2	3.0
44	10	5	3.4	1.4
45	11	5	4.0	1.6

purifying urban runoff, and for urban embellishment. In this study, a comprehensive approach has been introduced to determining the optimal areas of deployment of LID SCMs which relies on runoff simulation using SWMM coupled to multi-objective optimization to produce Pareto fronts of alternative solutions by considering three objectives and ranking of solutions with the TOPSIS method.

1. Objective 1: Reduction of stormwater overflows volume at flooding nodes inside the catchment and runoff volume at the catchment outlet to prevent flooding inside and downstream of the catchment respectively. Taken into account the reduction of runoff volume at the catchment outlet for cases where vulnerable urban areas exist downstream the catchment is of particular significance.
2. Objective 2: Cost minimization, which results in the most affordable alternative for the best performance of LID SCMs and the largest reduction in runoff volume, which is a key objective in most stormwater optimization problems due to financial limitations.
3. Objective 3: Minimize the service-performance reduction of LID SCMs considering this objective function improves their selection, assuring with longer-term performance. The third objective function improves the long term performance of designed alternatives is herein demonstrated by (1) comparing the results of the two-objective optimization without considering this objective function with the three-objective optimization results and (2) by comparing the results of the three-objective optimizations of two case studies in which the
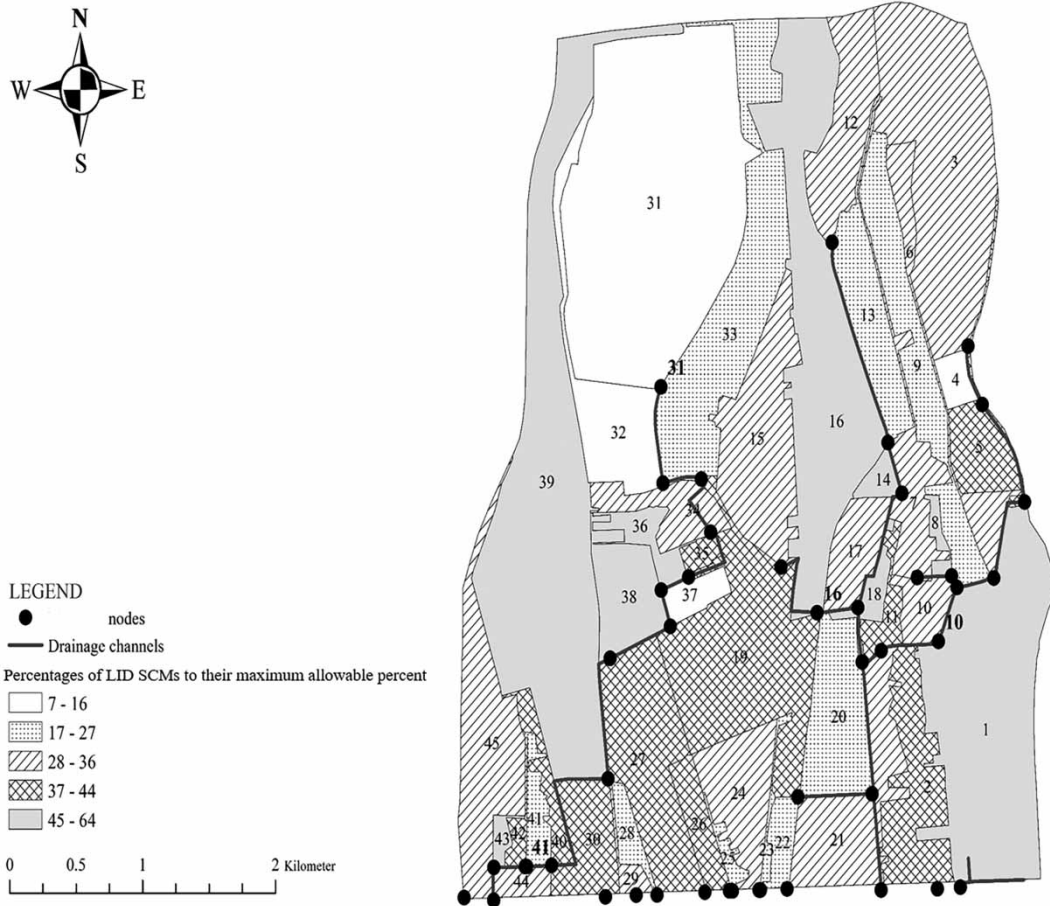
www.manaraa.com

Figure 7 │ Distribution of LID SCMs in the subcatchments of District 6.

Table 7 │ Magnitude of runoff volume and runoff volume reduction at selected nodes

Node no.	Overflow volume before applying LID SCMs (10^3 m³)	Overflow volume after applying LID SCMs (10^3 m³)	Reduced runoff volume (10^3 m³)	Fraction of reduced runoff volume (%)
10	6.55	1.38	5.17	78
16	30.64	16.445	14.20	46
31	33.40	21.15	12.25	37
41	1.07	0	1.07	100

Table 8 │ Runoff volume and peak discharge at the catchment outlet

Status	Peak discharge at outlet (10^3 m³/s)	Runoff volume at outfall (10^3 m³/s)	Time to peak flow (min)
Before applying LID SCMs	61.21	581.05	200
After applying LID SCMs	47.70	460.06	220

values of their first and second objective functions were approximately equal, while their third objective function value was significantly different, thus demonstrating the marginal value added by addition of the third objective.

The combination of porous pavement and bioretention cell as herein implemented to improve the performance of

Tehran's District 6 stormwater infrastructure whose results indicate the ability of these two LID SCMs to control runoff volume.

The MOALOA solved the three-objective optimization, and its results were compared with those of well-established NSGAII using 10 runs. The results show the superiority of MOALOA. Thus, the MOALOA was shown to be an effective algorithm in conjunction with SWMM for solving
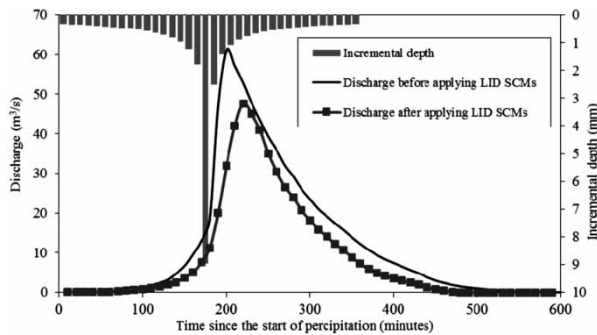
Figure 8 │ Outflow hydrograph before and after the application of LID SCMs.

complex multi-objective optimization problems involving LID SCMs deployment.

This study's approach was tested and successfully implemented with sample problems from the SWMM manual and with a catchment encompassing District 6 of Tehran municipality (Iran). The proposed simulation-optimization approach can assist stormwater experts the world over in choosing optimal combinations of LID SCMs with confidence to reduce urban flooding and improve water quality.

ACKNOWLEDGEMENTS

CONFLICTS OF INTEREST

None.

REFERENCES

Alsubih, M., Arthur, S., Wright, G. & Allen, D. 2017 Experimental study on the hydrological performance of a permeable pavement. *Urban Water Journal* **14** (4), 427–434.

Aminjavaheri, S. M. & Nazif, S. 2018 Determining the robust optimal set of BMPs for urban runoff management in data-poor catchments. *Journal of Environmental Planning and Management* **61** (7), 1180–1203.

Azarnivand, A. & Banihabib, M. E. 2016 A multi-level strategic group decision making for understanding and analysis of

sustainable watershed planning in response to environmental perplexities. *Group Decision and Negotiation*. doi: 10.1007/s10726-016-9484-8.

Baek, S. S., Choi, D. H., Jung, J. W., Lee, H. J., Lee, H., Yoon, K. S. & Cho, K. H. 2015 Optimizing low impact development (LID) for stormwater runoff treatment in urban area, Korea: experimental and modeling approach. *Water Research* **86** (1), 122–131.

Banihabib, M. E., Azarnivand, A. & Peralta, R. C. 2015 A new framework for strategic planning to stabilize a shrinking lake. *Lake and Reservoir Management* **31** (1), 31–43.

Barkdoll, B. D., Kantor, C. M., Wesseldyke, E. S. & Ghimire, S. R. 2016 Stormwater low-impact development: a call to arms for hydraulic engineers. *Journal of Hydraulic Engineering* **142** (8), 02516002.

Bozorg-Haddad, O., Azarnivand, A., Hosseini-Moghari, S. M. & Loáiciga, H. A. 2016 Development of a comparative multiple criteria framework for ranking Pareto optimal solutions of a multiobjective reservoir operation problem. *Journal of Irrigation and Drainage Engineering* **142** (7), 04016019.

Bozorg-Haddad, O., Solgi, M. & Loáiciga, H. A. 2017 *Meta-heuristic and Evolutionary Algorithms for Engineering Optimization*. John Wiley & Sons, Hoboken, New Jersey.

Brunetti, G., Šimůnek, J. & Piro, P. 2016 A comprehensive numerical analysis of the hydraulic behavior of a permeable pavement. *Journal of Hydrology* **540**, 1146–1161.

Cano, O. M. & Barkdoll, B. D. 2016 Multiobjective, socioeconomic, boundary-emanating, nearest distance algorithm for stormwater low-impact BMP selection and placement. *Journal of Water Resources Planning and Management* **143** (1), 05016013.

Carpenter, D. D. & Hallam, L. 2009 Influence of planting soil mix characteristics on bioretention cell design and performance. *Journal of Hydrologic Engineering* **15** (6), 404–416.

Central Bank of the Islamic Republic of Iran 2017 *Inflation Rate*. https://www.cbi.ir/ (accessed 5 January 2019).

Chau, H. F. 2009 *Green Infrastructure for Los Angeles: Addressing Urban Runoff and Water Supply through low Impact Development*. City of Los Angeles stormwater program, Los Angeles, California, USA, pp. 6–34.

Chui, T. F. M., Liu, X. & Zhan, W. 2016 Assessing cost-effectiveness of specific LID practice designs in response to large storm events. *Journal of Hydrology* **533** (1), 353–364.

Collins, K. A., Hunt, W. F. & Hathaway, J. M. 2009 Side-by-side comparison of nitrogen species removal for four types of permeable pavement and standard asphalt in eastern North Carolina. *Journal of Hydrologic Engineering* **15** (6), 512–521.

Damodaram, C. & Zechman, E. M. 2012 Simulation-optimization approach to design low impact development for managing peak flow alterations in urbanizing watersheds. *Journal of Water Resources Planning and Management* **139** (3), 290–298.

Davis, A. P. 2005 Green engineering principles promote low-impact development. *Journal of Environmental Science and Technology* **39** (16), 338A–344A.

Davis, A. P. 2008 Field performance of bioretention: hydrology impacts. *Journal of Hydrologic Engineering* **13** (2), 90–95.

www.manaraa.com

Davis, A. P., Hunt, W. F., Traver, R. G. & Clar, M. 2009 Bioretention technology: overview of current practice and future needs. *Journal of Environmental Engineering* **135** (3), 109–117.

Deo, O., Sumanasooriya, M. & Neithalath, N. 2010 Permeability reduction in pervious concretes due to clogging: experiments and modeling. *Journal of Materials in Civil Engineering* **22** (7), 741–751.

Dietz, M. E. 2007 Low impact development practices: a review of current research and recommendations for future directions. *Water, Air, and Soil Pollution* **186** (1–4), 351–363.

Dietz, M. E. & Clausen, J. C. 2008 Stormwater runoff and export changes with development in a traditional and low impact subdivision. *Journal of Environmental Management* **87** (4), 560–566.

Eckart, K. B. C. 2015 *Multiobjective Optimization of Low Impact Development Stormwater Controls Under Climate Change Conditions*. Master of Applied Science Thesis, Department of Civil and Environmental Engineering, University of Windsor, Windsor, Ontario, Canada.

Eckart, K., McPhee, Z. & Bolisetti, T. 2017 Performance and implementation of low impact development – A review. *Science of the Total Environment* **607**, 413–432.

Eckart, K., McPhee, Z. & Bolisetti, T. 2018 Multiobjective optimization of low impact development stormwater controls. *Journal of Hydrology* **562**, 564–576.

Emerson, C. H., Wadzuk, B. M. & Traver, R. G. 2010 Hydraulic evolution and total suspended solids capture of an infiltration trench. *Hydrological Processes: An International Journal* **24** (8), 1008–1014.

Fach, S., Engelhard, C., Wittke, N. & Rauch, W. 2011 Performance of infiltration swales with regard to operation in winter times in an Alpine region. *Water Science and Technology* **63** (11), 2658–2665.

Fallahi Zarandi, A. 2013 *Selection the Optimum Combination of Best Management Practices (BMPs) with Economic Considerations in Improving the Quality of Urban Runoff in Tehran*. PhD Dissertation, College of Engineering. Kharazmi University.

Fassman, E. A. & Blackbourn, S. 2010 Urban runoff mitigation by a permeable pavement system over impermeable soils. *Journal of Hydrologic Engineering* **15** (6), 475–485.

Freni, G. & Mannina, G. 2018 Long Term Efficiency Analysis of Infiltration Trenches Subjected to Clogging. In: *International Conference on Urban Drainage Modelling*, September 23–26, Palermo, Italy.

Gironás, J., Roesner, L. A., Davis, J., Rossman, L. & Supply, W. 2015 *Storm Water Management Model Applications Manual*. National Risk Management Research Laboratory, Office of Research and Development, US Environmental Protection Agency, Cincinnati, Ohio, USA.

Haselbach, L. M., Valavala, S. & Montes, F. 2006 Permeability predictions for sand-clogged Portland cement pervious concrete pavement systems. *Journal of Environmental Management* **81** (1), 42–49.

Haselbach, L., Dutra, V. F. P., Schwetz, P. & da Silva Filho, L. C. P. 2016 Laboratory Evaluations of Long-Term Hydraulic Performance and Maintenance Requirements for Pervious Concrete Mixes: A Case Study in Southern Brazil. In: *International Conference on Transportation and Development*, June 26–29, Houston, Texas, USA.

Hettiarachchi, S., Wasko, C. & Sharma, A. 2018 Increase in flood risk resulting from climate change in a developed urban watershed – the role of storm temporal patterns. *Hydrology and Earth System Sciences* **22** (3), 2041–2056.

Holman-Dodds, J. K., Bradley, A. A. & Potter, K. W. 2003 Evaluation of hydrologic benefits of infiltration based urban storm water management. *Journal of American Water Resources Association* **39** (16), 205–215.

Huang, J., He, J., Valeo, C. & Chu, A. 2016 Temporal evolution modeling of hydraulic and water quality performance of permeable pavements. *Journal of Hydrology* **533**, 15–27.

Hunt, W. F., Smith, J. T., Jadlocki, S. J., Hathaway, J. M. & Eubanks, P. R. 2008 Pollutant removal and peak flow mitigation by a bioretention cell in urban Charlotte, NC. *Journal of Environmental Engineering* **134** (5), 403–408.

Hwang, C. L. & Yoon, K. 1981 *Multiple Attribute Decision Making: Methods and Applications*. Springer-Verlag, New York.

Inanlu, B., Zahraei, B. & Ruzbahani, A. 2012 Solving multi-objective problems of water resources management by combining multi-criteria decision making methods TOPSIS and PSO. In: *The 5th National Conference and Exhibition on Environmental Engineering*, 18–19 November, Tehran, Iran (In Persian).

James, M. B. & Dymond, R. L. 2011 Bioretention hydrologic performance in an urban stormwater network. *Journal of Hydrologic Engineering* **17** (3), 431–436.

Jayasooriya, V. M. & Ng, A. W. M. 2014 Tools for modeling of stormwater management and economics of green infrastructure practices: a review. *Water, Air, and Soil Pollution* **225** (8), 1–20.

Jia, H., Lu, Y., Shaw, L. Y. & Chen, Y. 2012 Planning of LID–BMPs for urban runoff control: the case of Beijing Olympic Village. *Separation and Purification Technology* **84** (1), 112–119.

Kamali, M., Delkash, M. & Tajrishy, M. 2017 Evaluation of permeable pavement responses to urban surface runoff. *Journal of Environmental Management* **187** (1), 43–53.

Li, H. & Davis, A. P. 2008 Urban particle capture in bioretention media. II: theory and model development. *Journal of Environmental Engineering* **134** (6), 419–432.

Li, H., Sharkey, L. J., Hunt, W. F. & Davis, A. P. 2009 Mitigation of impervious surface hydrology using bioretention in North Carolina and Maryland. *Journal of Hydrologic Engineering* **14** (4), 407–415.

Limbrunner, J. F., Vogel, R. M., Chapra, S. C. & Kirshen, P. H. 2013 Classic optimization techniques applied to stormwater and nonpoint source pollution management at the watershed scale. *Journal of Water Resources Planning and Management* **139** (5), 486–491.

Line, D. E. & Hunt, W. F. 2009 Performance of a bioretention area and a level spreader-grass filter strip at two highway sites in North Carolina. *Journal of Irrigation and Drainage Engineering* **135** (2), 217–224.

Loáiciga, H. A., Sadeghi, K. M., Shivers, S. & Kharaghani, S. 2015 Stormwater control measures: optimization methods for sizing and selection. *Journal of Water Resources Planning and Management* **141** (9), 04015006.

Lucke, T. & Beecham, S. 2011 Field investigation of clogging in a permeable pavement system. *Building Research and Information* **39** (6), 603–615.

Lucke, T. & Nichols, P. W. 2015 The pollution removal and stormwater reduction performance of street-side bioretention basins after ten years in operation. *Science of the Total Environment* **536**, 784–792.

MahabGhods Consulting Engineering Company 2011a *Tehran Stormwater Management Master Plan*. Second volume, Basic studies, Tehran, Iran, pp. 232–241 (In Persian).

MahabGhods Consulting Engineering Company 2011b *Tehran Stormwater Management Master Plan*. Eleventh volume, Summary Reports, Tehran, Iran, pp. 232–241 (In Persian).

Management and Planning Organization of Iran 2017 *Unit Price List of Construction Field*. Number 94/449038, Tehran, Iran.

Mani, M., Bozorg-Haddad, O. & Chu, X. 2018 Ant Lion Optimizer (ALO) Algorithm. In: *Advanced Optimization by Nature-Inspired Algorithms* (O. Bozorg-Haddad, ed.). Springer, Singapore, pp. 105–116.

MATLAB 2012 [Computer software]. Natick, MA, MathWorks.

Mirjalili, S. 2015 The ant lion optimizer. *Advances in Engineering Software* **83** (1), 80–98.

Mirjalili, S., Jangir, P. & Saremi, S. 2017 Multi-objective ant lion optimizer: a multi-objective optimization algorithm for solving engineering problems. *Applied Intelligence* **45** (1), 1–17.

Montaseri, M., Hesami-Afshar, M. & Bozorg-Haddad, O. 2015 Development of simulation-optimization model (MUSIC-GA) for urban stormwater management. *Water Resources Management* **29** (13), 4649–4665.

Morsy, M. M., Goodall, J. L., Shatnawi, F. M. & Meadows, M. E. 2016 Distributed stormwater controls for flood mitigation within urbanized watersheds: case study of Rocky Branch watershed in Columbia, South Carolina. *Journal of Hydrologic Engineering* **21** (11), 05016025.

Osouli, A., Bloorchian, A. A., Grinter, M., Alborzi, A., Marlow, S. L., Ahiablame, L. & Zhou, J. 2017 Performance and cost perspective in selecting BMPs for linear projects. *Water* **9** (5), 302.

Palla, A. & Gnecco, I. 2015 Hydrologic modeling of low impact development systems at the urban catchment scale. *Journal of Hydrology* **528**, 361–368.

Pencheva, T., Atanassov, K. & Shannon, A. 2009 Modelling of a roulette wheel selection operator in genetic algorithms using generalized nets. *International Journal of Bioautomation* **13** (4), 257–264.

Pennsylvania Department of Environmental Protection (PaDEP) 2006 *Pennsylvania Stormwater Best Management Practices Manual*. Pennsylvania Department of Environmental Protection, Harrisburg, PA.

Pezzaniti, D., Beecham, S. & Kandasamy, J. 2009 Influence of clogging on the effective life of permeable pavements.

Proceedings of the Institution of Civil Engineers – Water Management **162** (3), 211–220.

Razzaghmanesh, M. & Beecham, S. 2018 A review of permeable pavement clogging investigations and recommended maintenance regimes. *Water* **10** (3), 337.

Rossman, L. A. 2015 *Storm Water Management Model User's Manual, Version 5.1*. National Risk Management Research Laboratory, Office of Research and Development, US Environmental Protection Agency, Cincinnati, Ohio, USA.

Sadeghi, M., Loáiciga, H. A. & Kharaghani, S. 2017 Stormwater control measures for runoff and water quality management in urban landscapes. *Journal of the American Water Resources Association* **54** (1), 124–133.

Sarzaeim, P., Bozorg-Haddad, O. & Chu, X. 2018 Teaching-Learning-Based Optimization (TLBO) Algorithm. In: *Advanced Optimization by Nature-Inspired Algorithms* (O. Bozorg-Haddad, ed.). Springer, Singapore, pp. 51–58.

Siriwardene, N. R., Deletic, A. & Fletcher, T. D. 2007 Clogging of stormwater gravel infiltration systems and filters: insights from a laboratory study. *Water Research* **41** (7), 1433–1440.

Tao, T., Wang, J., Xin, K. & Li, S. 2014 Multi-objective optimal layout of distributed storm-water detention. *International Journal of Environmental Science and Technology* **11** (5), 1473–1480.

Tehran University-Graduate Faculty of Environment 2015 *Application of SWMM in the Collection and Disposal of Urban Floods (Case Study: District 6 of Tehran Municipality)*. Tehran, Iran, 1–78 (In Persian).

Tobio, J. A. S., Maniquiz-Redillas, M. C. & Kim, L. H. 2015 Optimization of the design of an urban runoff treatment system using stormwater management model (SWMM). *Journal of Desalination and Water Treatment* **53** (11), 3134–3141.

Trinh, D. H. & Chui, T. F. M. 2013 Assessing the hydrologic restoration of an urbanized area via an integrated distributed hydrological model. *Hydrology and Earth System Sciences* **17** (12), 4789–4801.

US Dept. of Agriculture Soil Conservation Service (USDA SCS) 1986 *Urban Hydrology for Small Watersheds*. Technical Release, No. 55 (TR-55), Washington, DC.

Xu, Z. & Zhao, G. 2016 Impact of urbanization on rainfall-runoff processes: case study in the Liangshui River basin in Beijing, China. *Proceedings of the International Association of Hydrological Sciences* **373**, 7–12.

Yao, L., Wei, W. E. I., Yu, Y., Xiao, J. & Chen, L. 2018 Rainfall-runoff risk characteristics of urban function zones in Beijing using the SCS-CN model. *Journal of Geographical Sciences* **28** (5), 656–668.

York, C., Goharian, E. & Burian, S. J. 2015 Impacts of large-scale stormwater green infrastructure implementation and climate variability on receiving water response in the Salt Lake City area. *American Journal of Environmental Sciences* **11** (4), 278.

Zhang, S. & Guo, Y. 2014 Stormwater capture efficiency of bioretention systems. *Water Resources Management* **28** (1), 149–168.